Optimal modularity for nucleation in a network-organized Ising model

Hanshuang Chen and Zhonghuai Hou*
Hefei National Laboratory for Physical Sciences at Microscale, Department of Chemical Physics, University of Science and Technology of China, Hefei, 230026, China
(Received 18 January 2011; published 26 April 2011)

We study the nucleation dynamics of the Ising model in a topology that consists of two coupled random networks, thereby mimicking the modular structure observed in real-world networks. By introducing a variant of a recently developed forward flux sampling method, we efficiently calculate the rate and elucidate the pathway for the nucleation process. It is found that as the network modularity worsens the nucleation undergoes a transition from a two-step to one-step process. Interestingly, the nucleation rate shows a nonmonotonic dependence on the modularity, in which a maximal nucleation rate occurs at a moderate level of modularity. A simple mean-field analysis is proposed to qualitatively illustrate the simulation results.

DOI: 10.1103/PhysRevE.83.046124 PACS number(s): 89.75.Hc, 64.60.Q−, 05.50.+q

I. INTRODUCTION

In the last decade, critical phenomena in complex networks have received an enormous amount of attention in the field of statistical physics and many other disciplines (see [1] for a recent review). Extensive research interests have focused on the onset of critical behaviors in diverse network topology, including the percolation phenomenon [2–5], epidemic thresholds [6,7], order-disorder transitions [8–12], synchronization [13,14], self-organized criticality [15,16], and nonequilibrium pattern formation [17]. However, there is much less attention paid to the dynamics or kinetics of a phase transition itself in complex networks, such as nucleation in a first-order phase transition.

Nucleation is a fluctuation-driven process that initiates the decay of a metastable state into a more stable one [18]. A first-order phase transition usually involves the nucleation and growth of a new phase. Many important phenomena in nature, including crystallization [19], glass formation [20], and protein folding [21], are associated with nucleation. Despite its apparent importance, many aspects of the nucleation process are still unclear and deserve further investigation. The Ising model, which is a paradigm for many phenomena in statistical physics, has been widely used to study the nucleation process. Despite its simplicity, the Ising model has made important contributions to the understanding of the nucleation phenomena in equilibrium systems and is likely to yield important insights for nonequilibrium systems as well. In two-dimensional lattices, for instance, shear can enhance the nucleation rate and the rate peaks at an intermediate shear rate [22], a single impurity may considerably enhance the nucleation rate [23], the existence of a pore may lead to two-stage nucleation, and the overall nucleation rate can reach a maximum level at an intermediate pore size [24]. The nucleation pathway of the Ising model in three-dimensional lattices has also been studied using the transition path sampling approach [25]. In addition, the Ising model has been frequently used to test the validity of classical nucleation theory (CNT) [26–30]. However, all these studies are limited to regular lattices in Euclidean space. Since many real systems can be properly modeled by network-organized structure, it is natural to ask how the topology of a networked system affects the nucleation process of the Ising model.

In a recent work [31], we studied nucleation dynamics on scale-free networks, in which we found that nucleation starts from, on average, nodes with more lower degrees, the rate for nucleation decreases exponentially with network size, and the size of the critical nuclei increases linearly with network size, implying that nucleation is relevant only for a finite-size network. In this paper, we study the nucleation dynamics of the Ising model in a modular network composed of two coupled random networks. It has been found that many real-world networks, ranging from social networks to biological networks, exhibit modularity structures [32,33], that is, links within modules are much more dense than those between modules. Many previous studies have revealed that such modular structures have a significant impact on the dynamics taking place on the networks, such as synchronization [34,35], neural excitability [36], spreading dynamics [37,38], opinion formation [39,40], and Ising phase transition [41–43]. In particular, for the majority model [39] and the Ising model [41–43] in modular networks, it has been shown that there exists a region in a discontinuous transition where a modular order phase and a global order phase coexist. However, these studies mainly focused on phase diagrams in parameter space, and did not investigate the transition process in detail from one phase to another that may undergo a nucleation process.

Since nucleation is an activated process that occurs extremely slowly, a brute force simulation is prohibitively expensive. To overcome this difficulty, we used a variant of a recently developed simulation method, forward flux sampling (FFS) [44]. This method allows us to calculate the nucleation rate and determine the properties of the ensemble toward nucleation pathways. We found that as the degree of network modularity decreases, nucleation goes through a transition from a two-step to a one-step process, and the rate exhibits a maximum at an intermediate degree of modularity. Free energy profiles for different modularities obtained by umbrella sampling (US) [45] and a simple mean-field (MF) analysis help us understand the FFS results.

This paper is organized as follows. In Sec. II, we describe the details of our model and the simulation method applied

*hzhlj@ustc.edu.cn

to this system. In Sec. III, we present the results for the nucleation rate and pathway in modular networks. In Sec. IV, a simple mean-field analysis is used to qualitatively illustrate the simulation results. Finally, discussion and main conclusions are addressed in Sec. V.

II. MODEL AND SIMULATION DETAILS

Consider a network consisting of N nodes arranged into two modules with N_1 and N_2 nodes. For simplicity, we only consider the case of $N_1 = N_2 = N/2$ throughout this paper. The connection probability between a pair of nodes belonging to the same module is ρ_i, while that for nodes belonging to different modules is ρ_o. The parameter $\sigma = (\rho_o/\rho_i) \in [0,1]$, defined as the ratio of intermodular to intramodular connectivity, measures the degree of modularity. The higher the degree of modularity of a network is, the smaller the value of σ is. As $\sigma \to 0$, the network becomes two isolated clusters, while as $\sigma \to 1$, the network approaches an Erdös-Rényi (ER) random network. When σ is varied, the total number of links of the network is kept unchanged, $N\langle k\rangle/2$, where $\langle k\rangle$ is the average degree. This restriction leads to $\rho_i = 2\langle k\rangle/N(1+\sigma)$ and $\rho_o = 2\langle k\rangle\sigma/N(1+\sigma)$. Each node is endowed with an Ising spin variable s_i that can be either $+1$ (up) or -1 (down). The Hamiltonian of the system is given by

$$H = -J\sum_{i<j} a_{ij}s_i s_j - h\sum_i s_i, \tag{1}$$

where J (> 0) is the coupling constant and h is the external magnetic field. The elements of the adjacency matrix of the network take $a_{ij} = 1$ if nodes i and j are connected and $a_{ij} = 0$ otherwise.

Our simulation is performed by Metropolis spin-flip dynamics [46], in which we attempt to flip each spin once, on average, during each Monte Carlo (MC) cycle. In each attempt, a randomly chosen spin is flipped with the probability $\min(1, e^{-\beta\Delta E})$, where $\beta = 1/(k_B T)$ and k_B is the Boltzmann constant, T is the temperature, and ΔE is the energy difference due to the flipping process. Here, we set $J = 1, h > 0, T < T_c$ (T_c is the critical temperature), and start with a metastable state in which $s_i = -1$ for most of the spins. The system will stay in that state for a significantly long time before undergoing a nucleation transition to a more stable state with most spins pointing up. We are interested in the pathway and rate for this nucleation process.

The FFS method has been used to calculate rate constants and transition paths for rare events in equilibrium and nonequilibrium systems [22–24,44,47,48]. This method uses a series of interfaces in phase space between the initial and final states to force the system from the initial state A to the final state B in a ratchetlike manner. Before the simulation begins, an order parameter λ is first defined, such that the system is in state A if $\lambda < \lambda_0$ and it is in state B if $\lambda > \lambda_M$. A series of nonintersecting interfaces λ_i ($0 < i < M$) lie between states A and B, such that any path from A to B must cross each interface without reaching λ_{i+1} before λ_i. The algorithm first runs a long-time simulation which gives an estimate of the flux $\bar{\Phi}_{A,0}$ escaping from the basin of A and generates a collection of configurations corresponding to crossings of interface λ_0. The next step is to choose a configuration from this collection at random and use it to initiate a trial run which is continued until it either reaches λ_1 or returns to λ_0. If λ_1 is reached, the configuration of the end point of the trial run is stored. This step is repeated, each time choosing a random starting configuration from the collection at λ_0. The fraction of successful trial runs gives an estimate of the probability of reaching λ_1 without going back into A, $P(\lambda_1|\lambda_0)$. This process is repeated, step by step, until λ_M is reached, giving the probabilities $P(\lambda_{i+1}|\lambda_i)$ ($i = 1,\ldots,M-1$). Finally, we get the transition rate R from A to B, which is the product of the flux $\bar{\Phi}_{A,0}$ and the probability $P(\lambda_M|\lambda_0) = \prod_{i=0}^{M-1} P(\lambda_{i+1}|\lambda_i)$ of reaching λ_M from λ_0 without going into A. For detailed descriptions of the FFS method see Ref. [49].

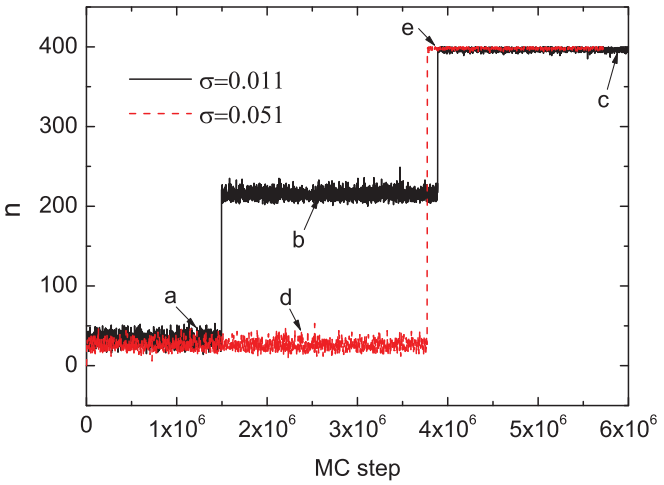

FIG. 1. (Color online) Typical time evolutions of the number of up spins λ. It is shown that the system undergoes a two-step nucleation process for $\sigma = 0.011$ and a one-step nucleation process for $\sigma = 0.051$. The representative network configurations at different moments indicated by arrows are shown in Fig. 2. Other parameters are $N = 400$, $\langle k\rangle = 6$, $T = 2.0$, and $h = 1.2$.

However, the conventional FFS method will become very inefficient if one intermediate metastable state exists between the initial state and final state, as a two-step nucleation process demonstrated in Fig. 1. This is because sampling paths will be trapped in these long-lived metastable states so that they rarely return to the initial state. To solve this problem, we perform two-step samplings from the initial down-spin state to the intermediate metastable state, then to the final up-spin state, giving the two-step rates, R_1 and R_2, respectively. Since the total mean time for nucleation is simply the sum of the mean time of the two-step process, the total rate can be expressed as $R = (R_1^{-1} + R_2^{-1})^{-1}$. To determine the location of the intermediate state we monitor the sampling time for the probability $P(\lambda_{i+1}|\lambda_i)$ between two neighboring interfaces during FFS. If the sampling time spent between interfaces i and $i+1$ is much more than its previous step and the probability $P(\lambda_{i+1}|\lambda_i)$ is nearly 1, we consider the ith interface as the location of the intermediate state. If such conditions are not met during the whole sampling, the intermediate metastable state does not exist, meaning that nucleation is a one-step process. Note that the method is straightforward to generalize to a multistep nucleation process.

Here, we define the order parameter λ as the total number of up spins in the networks. The spacing between interfaces is fixed at three up spins, but the computed results do not depend on this spacing. We perform 1000 trials per interface for each FFS sampling, from which at least 100 configurations are saved at each interface in order to investigate the statistical properties of an ensemble of reactive pathways to nucleation. The results are obtained by averaging over 10 independent FFS samplings and 50 different network realizations.

III. RESULTS

To begin with, in Fig. 1 we exhibit typical time evolutions of the number of up spins λ corresponding to two different values of network modularity $\sigma = 0.011$ and $\sigma = 0.051$ via brute-force simulations, with relevant parameters $N = 400$, $\langle k \rangle = 6$, $T = 2.0$, and $h = 1.2$. It is clearly observed that the system undergoes a two-step nucleation process for $\sigma = 0.011$ and a one-step nucleation process for $\sigma = 0.051$. We also plot several representative configurations in Fig. 2, corresponding to different phases of the system. Before the nucleation happens, the system lies in a metastable state, where most of the nodes are in down-spin state (indicated by blue circles), as shown in Fig. 2(a) and Fig. 2(d). When the network modularity is very good, the system enters into an intermediate metastable state via the first-step nucleation, where nodes in one of the modules are in the up-spin state (indicated by red triangles), while nodes in the other module are still in the down-spin state, as shown in Fig. 2(b). When the network modularity worsens, such an intermediate metastable state disappears so that the nucleation becomes a one-step process. Finally, the system will enter into the most stable state, where almost all spins are in the up-spin state, as shown in Fig. 2(c) and Fig. 2(e). Moreover, we note that that the nucleation process typically takes the order of 10^6 or more MC steps, which is computationally costly. Therefore, in what follows we will give the results obtained by the FFS method.

The nucleation rate R as a function of σ is plotted in Fig. 3(a), with relevant parameters being the same as those in Fig. 1 except for $h = 1.0$. One can see that as σ increases R reaches a maximum R_c at $\sigma \simeq 0.031$ and then decreases. Obviously, there exists a maximal nucleation rate that occurs at a moderate degree of network modularity. In Fig. 3(b), we plot the results of the nucleation rates, R_1 and R_2, for a two-step process as functions of σ. As σ increases, R_1 seems to exponentially decrease with σ, while R_2 increases monotonically until $\sigma = 0.051$ is reached. For $\sigma > 0.051$, nucleation becomes a one-step process so that R_2 can not be well defined and the overall nucleation rate is only determined by R_1. Figure 3(b) shows that R_2 is much lower than R_1 when the value of σ is relatively small, so that R is dominantly determined by the second step nucleation. While for $\sigma > 0.031$, R is determined almost exclusively by the first step nucleation. Thus, there exists a region $0.001 < \sigma < 0.031$ where R is determined by both R_1 and R_2. Note that we have also made extensive simulations for other parameters such as $h = 0.7, 1.2$ and $T = 1.5, 1.8$, and found that the qualitative features of the above results do not change (results not shown).

To further understand the above results, we calculate the free energy of the system using the US method, in which we use a bias potential $0.1 k_B T(\lambda - \bar{\lambda})^2$, with $\bar{\lambda}$ being the center of each window. The free energy ΔF as a function of λ for three different values of σ are depicted in Fig. 4(a). For $\sigma = 0.001$ and $\sigma = 0.031$, there are two free-energy maximums, occurring at the locations of the critical nuclei $\lambda = \lambda_1^*$ and

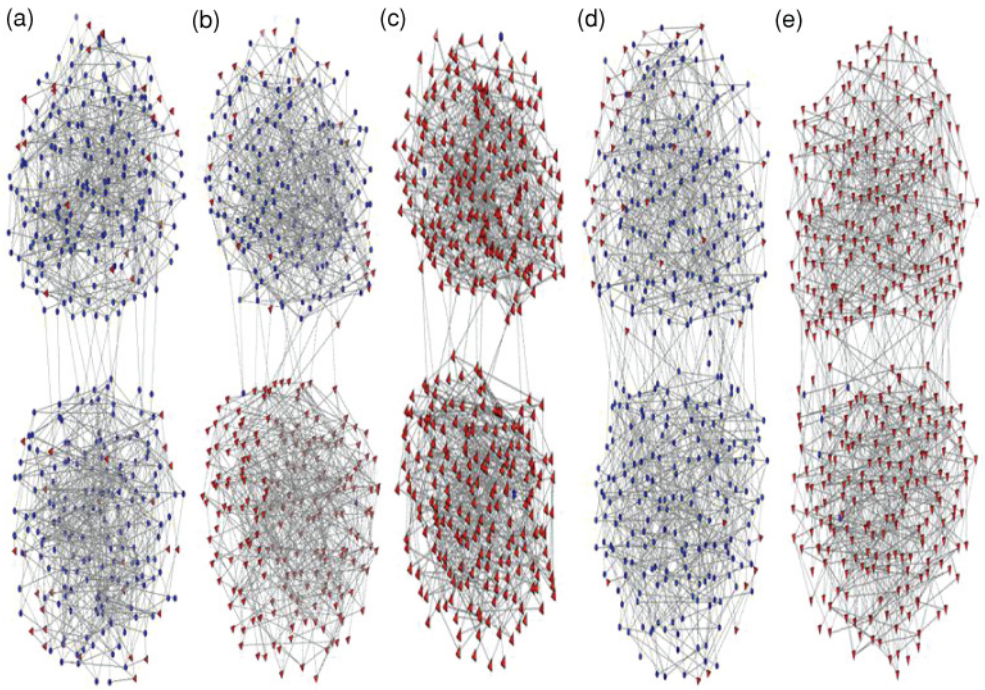

FIG. 2. (Color online) Five representative network configurations at different moments indicated in Fig. 1, where down-spin nodes and up-spin nodes are denoted by blue circles and red triangles, respectively. (a)–(c) correspond to the case of $\sigma = 0.011$ and (d),(e) correspond to the case of $\sigma = 0.051$.

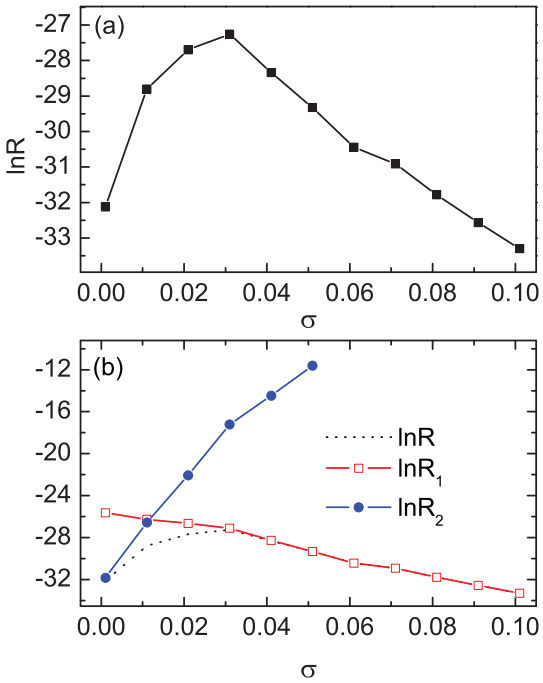

FIG. 3. (Color online) (a) The logarithm of the nucleation rate $\ln R$ as a function of the degree of modularity σ. (b) $\ln R_1$ (squares) and $\ln R_2$ (circles) as a function of σ, and dotted line indicates the overall rate $\ln R$. The parameters are same as in Fig. 1 except for $h = 1.0$.

$\lambda = \lambda_2^*$, respectively. This picture is consistent with the two-step nucleation process described previously. For a larger $\sigma = 0.101$, only the first free-energy barrier is present, implying that the nucleation becomes a one-step process. With each increment of σ, λ_1^* moves to a larger value while the value of λ_2^* gets smaller, as shown in Fig. 4(b). Figure 4(c) shows that the first free-energy barrier ΔF_1^*, defined as the difference between the free energy at λ_1^* and the first minimum in free energy ($\lambda = 23$), increases almost linearly with σ, while the second free-energy barrier ΔF_2^* (defined similarly to ΔF_1^*, and the second minimum in free energy is an increasing function of σ, within the range $\lambda \in [78,93]$) decreases monotonically with σ until ΔF_2^* vanishes at $\sigma > 0.051$, which is in agreement with the result of Fig. 3(b).

IV. MEAN-FIELD ANALYSIS

In order to unveil the possible mechanism behind the above phenomenon, we present an analytical understanding by CNT and simple MF approximation. First, for the first-step nucleation, let us assume that λ nodes are in up spins and the remaining nodes are in down spins in one of modules (say module I for convenience), and all the nodes in the other module (module II) are in down spins. The energy change due to the spin flip of these λ nodes can be expressed as the sum of two parts $\Delta U_1 = -2h\lambda + 2JN_1^{\text{in}}$, where the first part denotes the energy loss due to the creation of λ up spins, which favors the growth of the nucleus, while the second part denotes the energy gain due to the formation of N_1^{in} new interfacial links between up and down spins, which does not favor the growth of the nucleus. According to the MF approximation, N_1^{in} can be

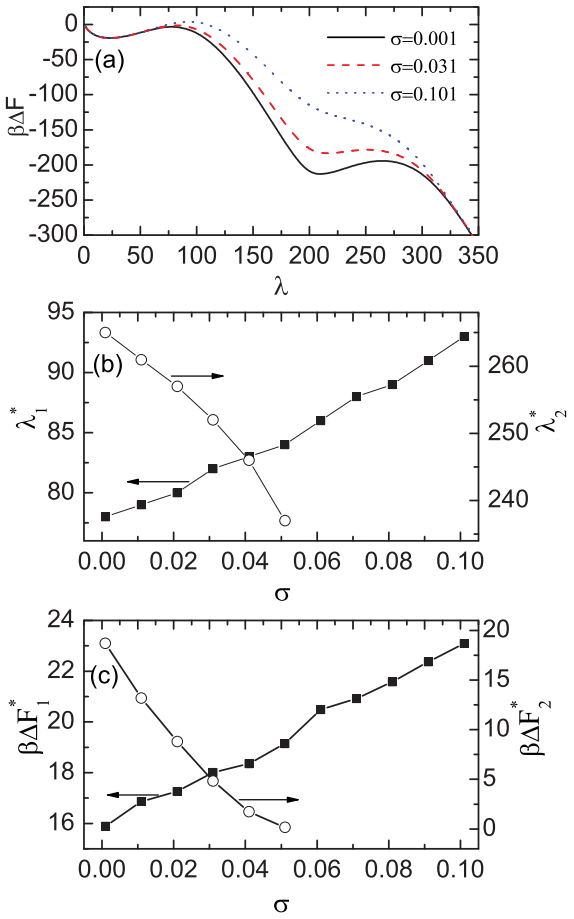

FIG. 4. (Color online) (a) Free energy ΔF as a function of λ for three different $\sigma = 0.001, 0.031, 0.101$. For smaller σ two free-energy barriers are clearly observed, while for larger σ the second one vanishes. (b) The size of the critical nuclei λ_1^* and λ_2^*, and (c) the free-energy barriers ΔF_1^* and ΔF_2^*, as functions of σ. The other parameters are the same as Fig. 2.

written as $N_1^{\text{in}} = \rho_i\lambda(N/2 - \lambda) + \rho_o\lambda(N/2)$, where the first part and the second part arise from interfacial links inside module I and between modules, respectively. For the second-step nucleation, we assume that all the nodes in module I are in up spins, and λ nodes in module II are in up spins while the remaining nodes are in down spins. This process creates new interfacial links inside module II, and at the same time removes old interfacial links between module I and module II. Thus, the energy change for this process is $\Delta U_2 = -2h\lambda + 2JN_2^{\text{in}}$ where $N_2^{\text{in}} = \rho_i\lambda(N/2 - \lambda) - \rho_o\lambda(N/2)$ is the net number of interfacial links. The entropy changes for the two nucleation processes are both

$$\Delta S = -\frac{k_B N}{2}\left[\frac{2\lambda}{N}\ln\left(\frac{2\lambda}{N}\right) + \left(1 - \frac{2\lambda}{N}\right)\ln\left(1 - \frac{2\lambda}{N}\right)\right].$$

Then, the changes of free energy for the two-step processes are $\Delta F_i = \Delta U_i - T\Delta S$ $(i = 1,2)$. In Fig. 5 we give the analytical results of the critical nuclei and free-energy barriers as functions of the network modularity. Clearly, the analysis agrees qualitatively with the simulation results of Fig. 4. From Fig. 5, one can see that with the increment of σ the size of

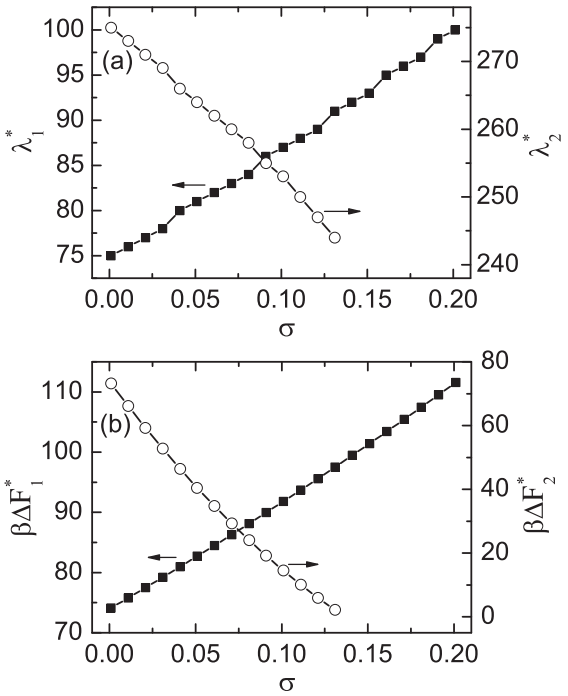

FIG. 5. The results of mean-field analysis. (a) The size of the critical nuclei λ_1^* and λ_2^*, and (b) the free-energy barriers ΔF_1^* and ΔF_2^*, as functions of σ. The other parameters are the same as Fig. 2.

the first critical nucleus and the height of the first free-energy barrier increase almost linearly, while the size of the second critical nucleus and the height of the second free-energy barrier decrease until $\sigma \simeq 0.13$ is reached. This implies that the analysis also predicts the extinction of the second nucleation stage, but this prediction obviously overestimates the transition value of σ.

V. CONCLUSIONS

In conclusion, we have studied the nucleation dynamics of the Ising model in modular networks consisting of two random networks. Using the FFS method, we found that as the network modularity gradually worsens a transition occurs from a one-step to a two-step nucleation process. Interestingly, the nucleation rate is a nonmonotonic function of the degree of modularity and a maximal rate exists for an intermediate level of modularity. Using the US method, we obtained free-energy profiles at different network modularities, from which one can see that two free-energy barriers exist for very good modularity while the second one vanishes as the network modularity worsens. This picture further confirms the FFS results. Finally, a mean-field analysis is employed to understand the nature of nucleation in modular networks and the simulation results. Since stochastic fluctuation and the coexistence of multistates are ubiquitous in social and biological systems, our study may provide valuable insights into fluctuation-driven transition phenomena that take place in network-organized systems with modular structures.

ACKNOWLEDGMENTS

This work was supported by the National Natural Science Foundation of China (Grants No. 20933006 and No. 20873130).

[1] S. N. Dorogovtsev, A. V. Goltseve, and J. F. F. Mendes, Rev. Mod. Phys. **80**, 1275 (2008).
[2] R. Cohen, K. Erez, D. ben-Avraham, and S. Havlin, Phys. Rev. Lett. **85**, 4626 (2000).
[3] D. S. Callaway, M. E. J. Newman, S. H. Strogatz, and D. J. Watts, Phys. Rev. Lett. **85**, 5468 (2000).
[4] M. E. J. Newman, Phys. Rev. Lett. **89**, 208701 (2002).
[5] R. Cohen, D. ben-Avraham, and S. Havlin, Phys. Rev. E **66**, 036113 (2002).
[6] R. Pastor-Satorras and A. Vespignani, Phys. Rev. Lett. **86**, 3200 (2001).
[7] C. Castellano and R. Pastor-Satorras, Phys. Rev. Lett. **105**, 218701 (2010).
[8] A. Aleksiejuk, J. A. Holysta, and D. Stauffer, Physica A **310**, 260 (2002).
[9] G. Bianconi, Phys. Lett. A **303**, 166 (2002).
[10] S. N. Dorogovtsev, A. V. Goltsev, and J. F. F. Mendes, Phys. Rev. E **66**, 016104 (2002).
[11] M. Leone, A. Vázquez, A. Vespignani, and R. Zecchina, Eur. Phys. J. B **28**, 191 (2002).
[12] C. P. Herrero, Phys. Rev. E **69**, 067109 (2004).
[13] T. Nishikawa, A. E. Motter, Y.-C. Lai, and F. C. Hoppensteadt, Phys. Rev. Lett. **91**, 014101 (2003).
[14] J. Gómez-Gardeñes, Y. Moreno, and A. Arenas, Phys. Rev. Lett. **98**, 034101 (2007).
[15] K. I. Goh, D.-S. Lee, B. Kahng, and D. Kim, Phys. Rev. Lett. **91**, 148701 (2003).
[16] A. E. Motter and Y. C. Lai, Phys. Rev. E **66**, 065102 (2002).
[17] H. Nakao and A. S. Mikhailov, Nature Phys. **6**, 544 (2010).
[18] D. Kashchiev, *Nucleation: Basic Theory with Applications* (Butterworth-Heinemann, Oxford, 2000).
[19] L. Gránásy and F. Iglói, J. Chem. Phys. **107**, 3634 (1997).
[20] G. Johnson, A. I. Melćuk, H. Gould, W. Klein, and R. D. Mountain, Phys. Rev. E **57**, 5707 (1998).
[21] A. R. Fersht, Proc. Natl. Acad. Sci. USA **92**, 10869 (1995).
[22] R. J. Allen, C. Valeriani, S. Tanase-Nicola, P. R. ten Wolde, and D. Frenke, J. Chem. Phys. **129**, 134704 (2008).
[23] R. P. Sear, J. Phys. Chem. B **110**, 4985 (2006).
[24] A. J. Page and R. P. Sear, Phys. Rev. Lett. **97**, 065701 (2006).
[25] A. C. Pan and D. Chandler, J. Phys. Chem. B **108**, 19681 (2004).
[26] M. Acharyya and D. Stauffer, Eur. Phys. J. B **5**, 571 (1998).

[27] V. A. Shneidman, K. A. Jackson, and K. M. Beatty, J. Chem. Phys. **111**, 6932 (1999).
[28] S. Wonczak, R. Strey, and D. Stauffer, J. Chem. Phys. **113**, 1976 (2000).
[29] K. Brendel, G. T. Barkema, and H. van Beijeren, Phys. Rev. E **71**, 031601 (2005).
[30] S. Ryu and W. Cai, Phys. Rev. E **81**, 030601(R) (2010).
[31] H. Chen, C. Shen, Z. Hou, and H. Xin, Phys. Rev. E **83**, 031110 (2011).
[32] M. E. J. Newman, Proc. Natl. Acad. Sci. USA **103**, 8577 (2006).
[33] S. Fortunato, Phys. Rep. **486**, 75 (2010).
[34] A. Arenas, A. Díaz-Guilera, and C. J. Pérez-Vicente, Phys. Rev. Lett. **96**, 114102 (2006).
[35] D. Li, I. Leyva, J. A. Almendral, I. Sendiña-Nadal, J. M. Buldú, S. Havlin, and S. Boccaletti, Phys. Rev. Lett. **101**, 168701 (2008).
[36] C. Zhou, L. Zemanová, G. Zamora, C. C. Hilgetag, and J. Kurths, Phys. Rev. Lett. **97**, 238103 (2006).
[37] Z. Liu and B. Hu, Europhys. Lett. **72**, 315 (2005).
[38] L. Huang, K. Park, and Y.-C. Lai, Phys. Rev. E **73**, 035103 (2006).
[39] R. Lambiotte and M. Ausloos, J. Stat. Mech. (2007) P08026.
[40] R. Lambiotte, M. Ausloos, and J. A. Hołyst, Phys. Rev. E **75**, 030101 (2007).
[41] R. K. Pan and S. Sinha, Europhys. Lett. **85**, 68006 (2009).
[42] S. Dasgupta, R. K. Pan, and S. Sinha, Phys. Rev. E **80**, 025101(R) (2009).
[43] K. Suchecki and J. A. Hołyst, Phys. Rev. E **80**, 031110 (2009).
[44] R. J. Allen, P. B. Warren, and P. R. ten Wolde, Phys. Rev. Lett. **94**, 018104 (2005).
[45] J. S. van Duijneveldt and D. Frenkel, J. Chem. Phys. **96**, 15 (1992).
[46] D. P. Landau and K. Binder, *A Guide to Monte Carlo Simulations in Statistical Physics* (Cambridge University Press, Cambridge, 2000).
[47] C. Valeriani, R. J. Allen, M. J. Morelli, D. Frenkel, and P. R. ten Wolde, J. Chem. Phys. **127**, 114109 (2007).
[48] R. J. Allen, D. Frenkel, and P. R. ten Wolde, J. Chem. Phys. **124**, 024102 (2006).
[49] R. J. Allen, C. Valeriani, and P. R. ten Wolde, J. Phys.: Condens. Mat. **21**, 463102 (2009).